ADVANCED FUNCTIONAL MATERIALS
www.afm-journal.de

www.MaterialsViews.com

A Near-Infrared *cis*-Configured Squaraine Co-Sensitizer for High-Efficiency Dye-Sensitized Solar Cells

*Chuanjiang Qin, Youhei Numata, Shufang Zhang, Ashraful Islam, Xudong Yang, Keitaro Sodeyama, Yoshitaka Tateyama, and Liyuan Han**

A *cis*-configured squaraine dye (HSQ1), synthesized by incorporation of a strongly electron-withdrawing dicyanovinyl group into the central squaric acid moiety, is employed in dye-sensitized solar cells (DSCs). In solution, HSQ1 displays an intense absorption in the near-infrared region with a maximum at 686 nm and when the dye is adsorbed on a TiO_2 surface, the absorption spectrum broadens in both the blue and the near-infrared regions, which is favorable for efficient light harvesting over a broad wavelength range. A solar cell sensitized with HSQ1 shows a broader incident photon-to-current conversion efficiency (IPCE) spectrum (from 400 to 800 nm) and a higher IPCE in the long-wavelength region (71% at 700 nm) than a cell sensitized with squaraine dye SQ1. Furthermore, a solar cell co-sensitized with HSQ1 and N3 dye shows remarkably improved short-circuit current density and open-circuit voltage compared to those of a DSC based on N3 alone and fabricated under the same conditions. The energy-conversion efficiency of the co-sensitized DSC is 8.14%, which is the highest reported efficiency for a squaraine dye–based co-sensitized DSC without using Al_2O_3 layer.

1. Introduction

Dye-sensitized solar cells (DSCs) have been receiving increasing attention as next-generation renewable energy sources because of their low cost of production.[1] To increase DSC efficiency by panchromatically harvesting solar light, researchers have focused great effort on developing dyes with absorption spectra that extend into the near-infrared (NIR) region.[2] However, designing a dye that absorbs sunlight efficiently from the visible to the NIR region is difficult. An alternative method for achieving panchromatic sensitization, called the dye cocktail method, involves the use of two dyes with complementary spectral coverages.[3] Most of the high-efficiency co-sensitized DSCs produced to date have combined black dye or a porphyrin dye with small-molecule organic dyes with large molar extinction coefficients (ε) in the UV or visible region, to compensate for the valley in that region of the incident photon-to-current conversion efficiency (IPCE) spectrum.[4] Co-sensitization with a NIR dye is expected to further extend the photoresponse region and thereby improve the efficiency of dye-cocktail DSCs. However, only a few appropriate NIR dyes are currently available for this purpose. Most of the existing NIR dyes have weak light absorption, insufficient IPCE response at long wavelengths, or both; and DSCs sensitized with NIR dyes tend to have a low open-circuit voltage (V_{OC}), which results in deterioration of DSC performance.[5]

Squaraine dyes are the most promising candidates as NIR co-sensitizers because of their extra-high ε and high IPCE in the NIR region.[6] For example, the squaraine dye SQ1 ($\varepsilon \approx 290\,000\ M^{-1}\ cm^{-1}$ at 647 nm, **Scheme 1**) has been used in dye-cocktail DSCs to enhance the IPCE response at long wavelengths.[7] However, the wavelength of absorption is still too short to compensate for the weak absorption in the NIR region. In attempts to bathochromically shift the absorption maximum, researchers have extended the π-conjugated structure of squaraine.[8] However, such extended structures are subject to serious unfavorable intermolecular aggregation on the TiO_2 surface. In addition, the extended structure is likely to cause competitive adsorption of dyes, which makes such structures unsuitable for co-sensitizing applications. Recently, a *cis*-configured squaraine dye was synthesized in an attempt to increase light absorption in the blue region via functionalizing the squaraine core with a weakly electron-withdrawing diethylbarbituric substitute. A solar cell sensitized with the dye shows a slightly higher energy-conversion efficiency (η) than a SQ1-sensitized cell.[9] However, the IPCE in the 600–700 nm region is only around 50%, which is not high enough for an efficient NIR co-sensitizer.

In this study, we designed and synthesized a new *cis*-configured squaraine dye, designated HSQ1, with a strongly electron-withdrawing dicyanovinyl substituent on the squaric acid core; HSQ1 exhibited a high IPCE response in the NIR region and molecular properties that made it a suitable

Dr. C. Qin, Dr. Y. Numata, Dr. S. Zhang,
Dr. A. Islam, Dr. X. Yang, Dr. L. Han
Photovoltaic Materials Unit and NIMS
Saint-Gobain Center of Excellence for Advanced Materials
National Institute for Materials Science
Sengen 1-2-1, Tsukuba, Ibaraki, 305-0047, Japan
E-mail: HAN.Liyuan@nims.go.jp
Dr. K. Sodeyama, Dr. Y. Tateyama
Nano-System Computational Science Group
Nano-Interface Unit
International Center for Materials Nanoarchitectonics
National Institute for Materials Science
Namiki 1-1, Tsukuba, Ibaraki, 305-0044, Japan

DOI: 10.1002/adfm.201203384

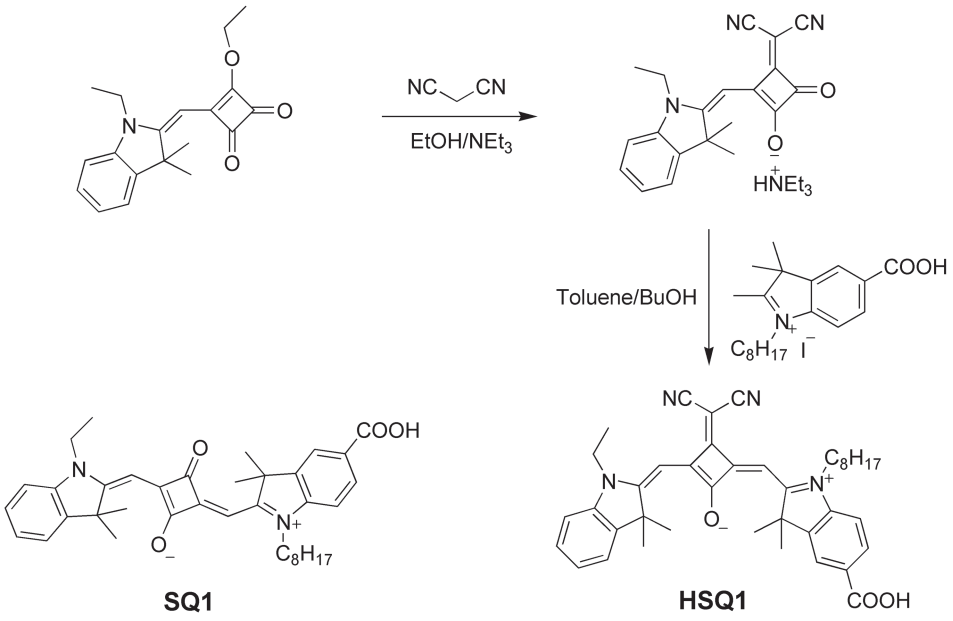

Scheme 1. Synthesis of HSQ1 and structure of SQ1.

co-sensitizer for DSCs with high energy-conversion efficiency. As expected, in the solution spectrum of HSQ1, the absorption maximum was remarkably red-shifted (by 39 nm) compared with that of SQ1, and a strong absorption at around 385 nm was also observed. When HSQ1 was adsorbed on TiO_2, the absorption spectrum broadened in both the blue and the NIR regions. A DSC based on HSQ1 performed much better than an SQ1-based DSC under the same conditions. The IPCE of the former was approximately 70% in the wavelength range from 630 to 710 nm, with a maximum of 71% at 700 nm. Furthermore, when HSQ1 was used as a co-sensitizer with N3 dye (a Ru bipyridyl complex), the resulting DSC was approximately 25% more efficient than a DSC based on N3 alone, and both the short-circuit current density (J_{SC}) and the open-circuit voltage (V_{OC}) were improved. We investigated possible explanations for the impressive performance of the co-sensitized DSC, and we propose a possible mechanism for improvement of the performance of solar cells by co-sensitization with N3 and HSQ1 dyes.

2. Results and Discussion

2.1. Synthesis

HSQ1 was synthesized by refluxing triethylammonium 2-[(1-ethyl-3,3-dimethyl-1,3-dihydro-2*H*-indol-2-ylidene)methyl]-3-(dicyanomethylidene)-4-oxocyclobut-1-en-1-olate and 5-carboxyl-2,3,3-trimethyl-1-octyl-3*H*-indolium in a 1:1 mixture of toluene and *n*-butanol. The condensation reaction afforded HSQ1 in 75% yield as a highly pure, air-stable, violet solid, which was fully characterized by ^{1}H and ^{13}C NMR spectroscopy, elemental analysis, and high-resolution mass spectrometry. HSQ1 was highly soluble in common organic solvents such as chloroform, dimethylformamide (DMF), and acetonitrile. Most methods for extending π-conjugation in squaraine dyes and thereby achieving

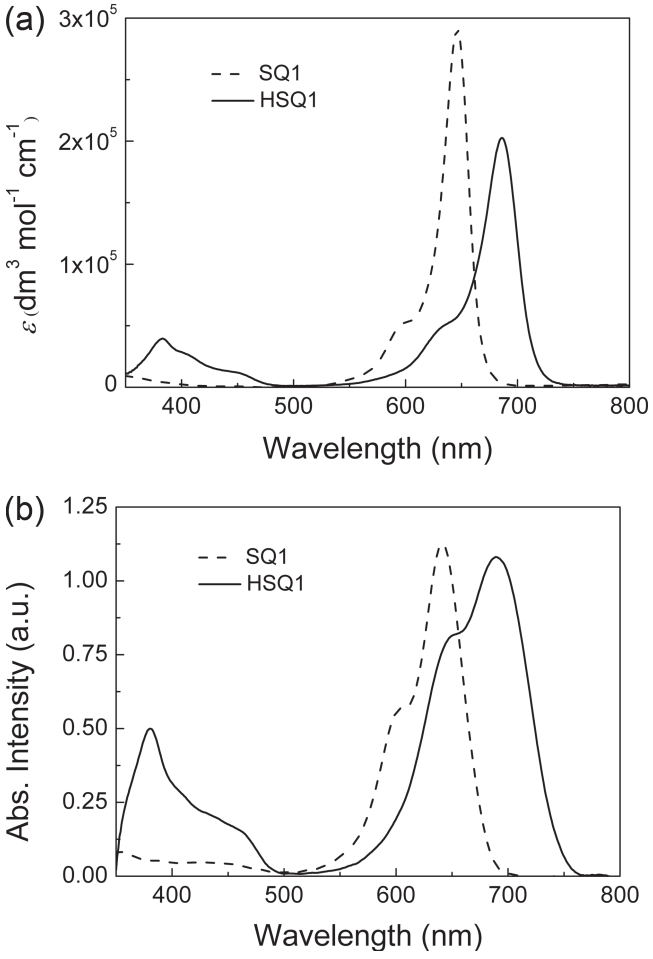

Figure 1. Absorption spectra of HSQ1 and SQ1 in DMF (left) and on TiO_2 (right; film thickness was 3.5 μm).

panchromatic absorption require many complex steps, whereas our simple synthetic strategy required only a few steps.

2.2. Absorption Spectroscopy

In DMF solution, HSQ1 showed two main absorption peaks, at 385 and 686 nm (ε = 39 300 and 202 000 M^{-1} cm^{-1}, respectively; **Figure 1**). We assigned the latter peak to the S_1 transition and the former peak to the higher-energy S_2 transition.[10] The λ_{max} of the S_1 transition was remarkably red-shifted (by 39 nm) relative to that of SQ1, and we attributed this shift to the strongly electron-withdrawing dicyanovinyl moiety on the central squaric acid. The intense absorption at 385 nm corresponding to the S_2 transition of HSQ1 was absent from the spectrum of SQ1.

When SQ1 was adsorbed onto a transparent TiO_2 electrode, the λ_{max} was blue-shifted by 6 nm, owing to interaction between the dye and the TiO_2; in addition, the shoulder peak underwent a red-shift of 8 nm and increased in intensity, owing to π–π aggregation (Figure 1). In contrast, when HSQ1 was adsorbed on TiO_2, the peak for the S_1 transition shifted bathochromically relative to the corresponding peak in the solution spectrum (from 686 nm in solution to 690 nm on TiO_2); in addition, a stronger π–π absorption in the high-energy region and a shoulder absorption around 650 nm were observed. These spectral features resulted in coverage of a wider range of solar radiation wavelengths and extended the absorption spectrum into the NIR region. Note that the absorption intensity of HSQ1 was similar to that of SQ1 at λ_{max} when the two dyes were adsorbed on TiO_2 films of the same thickness, even though the ε of the former was 17.2% lower than that of the latter in the solution. This result suggests that the loading amount of HSQ1 was much higher than that of SQ1.

2.3. Electrochemical Properties

HSQ1 exhibited reversible oxidative and reductive waves with half-wave potentials ($E_{1/2}$) at 0.93 and –0.53 V (vs. normal hydrogen electrode (NHE); **Figure 2**), whereas the corresponding values for SQ1 are 0.98, and –0.78 V, respectively.[6a] These differences in electrochemical properties suggest that the electron-withdrawing dicyanovinyl moiety substantially decreased the reduction potential of HSQ1 and narrowed the band gap with respect to that of SQ1. The oxidation potential of HSQ1 was low enough for efficient regeneration of the oxidized dye via electron donation from iodide (≈0.4 V vs. NHE).[11] From the intersection of the normalized absorption and fluorescence spectra (Figure S1, Supporting Information), the optical energy gap ($E_{0\text{-}0}$) of HSQ1 was determined to be 1.79 eV, and from this value, we calculated the excited state oxidation potential of HSQ1 to be –0.86 V (vs. NHE). The fact that this potential was much more negative than the conduction-band energy of TiO_2, which is approximately –0.5 V vs. NHE,[12] indicates that the driving force was sufficient for electron injection from the excited state of the sensitizer to the TiO_2 conduction band.

2.4. Computational Analysis of Structure and Electron Distribution

In the SQ1 dye, the donor groups are in a *trans* arrangement around the central squaric carbonyl group, whereas in HSQ1, the donor groups are in a *cis* arrangement in which there is no steric repulsion between the dicyano group and the dimethyl groups on the indolium moieties. To gain deeper insight into the molecular geometry and electronic structure of HSQ1, we used density functional theory (DFT) to calculate the dye's frontier molecular orbital distributions and optimized molecular structure (**Figure 3**). The calculations revealed that the highest occupied molecular orbital (HOMO) and the HOMO–1 orbital were distributed over the dicyanovinyl and squaraine units and extended partly to the indolium moieties. When the dye was adsorbed on the TiO_2 surface, the dicyanovinyl moiety (HOMO component) was exposed to the electrolyte directly in large degree, which could easily accept electrons from redox mediators for regeneration. The lowest unoccupied molecular orbital (LUMO) and the LUMO+1 orbital of HSQ1 were distributed

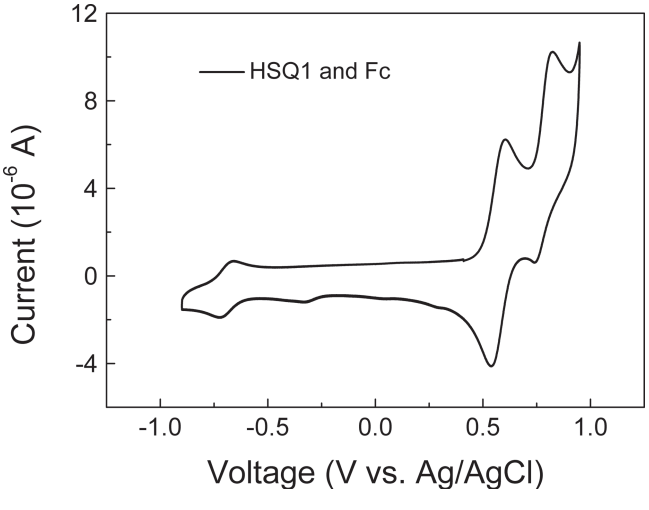

Figure 2. Cyclic voltammogram of HSQ1 in DMF with ferrocene (Fc) as an internal standard.

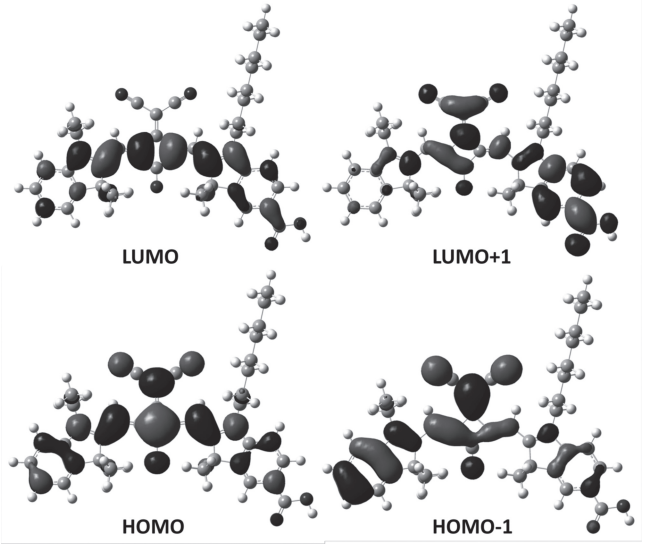

Figure 3. Calculated molecular orbitals of HSQ1.

Table 1. Selected results of time-dependent DFT calculations of the excited state transitions of HSQ1. The B3LYP/6-31G(d) basis set was used with the conductor-like polarized continuum model to take into account the effect of the DMF solvent.

State	Excitation energy [eV]	Oscillator strength *f*	Main MO transitions with their probabilities	
1	1.9907	1.2311	HOMO -> LUMO	(99.6%)
2	2.9412	0.5613	HOMO–2 -> LUMO	(3.3%)
			HOMO–1 -> LUMO	(95.0%)
3	3.3318	0.4494	HOMO–2 -> LUMO	(41.4%)
			HOMO–1 -> LUMO	(2.1%)
			HOMO -> LUMO+1	(38.8%)
			HOMO -> LUMO+2	(14.9%)

over the conjugated backbone and the carboxylic acid unit, respectively. These electron distributions facilitated electron injection from the photoexcited sensitizer dye to TiO_2 via the indolium associated with the anchoring carboxylic acid, because the electron-withdrawing dicyanovinyl unit of HSQ1 did not limit electron injection.

The absorption spectra and relative oscillator strengths (*f*) of HSQ1 and SQ1 calculated by time-dependent DFT were consistent with the corresponding experimental results (Figure S2 and Table S1, Supporting Information). The lowest-lying electronic transition of HSQ1 was from the HOMO to the LUMO, and this transition was red-shifted by approximately 40 nm compared with that of SQ1. The strongly electron-withdrawing dicyanovinyl group simultaneously raised the HOMO energy and decreased the LUMO energy, narrowing the band gap. The higher-energy electronic transitions in the blue region involved a combination of the HOMO–1 to LUMO transition (95.0%) and the HOMO–2 to LUMO transition (3.3%), as shown in **Table 1**. The absorption in the UV region was attributed mainly to the HOMO–2 to LUMO, HOMO to LUMO+1, and HOMO to LUMO+2 transitions. These three transitions were contributed to the effect of the dicyanovinyl group on the central squaric acid on the electron distribution.

2.5. Photovoltaic Performance of DSCs Based on HSQ1

The photovoltaic parameters of solar cells sensitized with SQ1 and HSQ1 under standard AM 1.5G simulated solar irradiation[13] are presented in **Table 2**, and their current

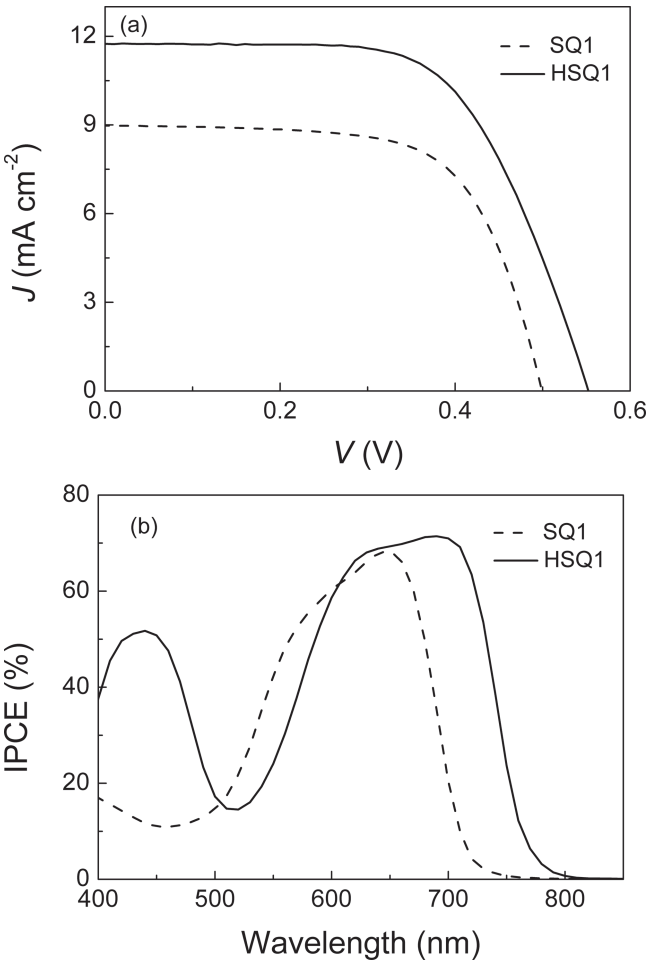

Figure 4. a) *J–V* curves and b) IPCE spectra for DSCs sensitized with HSQ1 and SQ1 in an electrolyte composed of 0.6 $_M$ dimethylpropylimidazolium iodide, 0.05 $_M$ I_2, and 0.1 $_M$ LiI in acetonitrile.

density–voltage (*J-V*) curves and IPCE spectra are presented in **Figure 4**. The HSQ1-sensitized cell showed higher J_{SC} and V_{OC} values (11.84 mA cm^{-2} and 0.55 V) than the SQ1-sensitized DSC (8.98 mA cm^{-2} and 0.50 V). The substantial increase of J_{SC} (31.8%) of the HSQ1-based cell was in good accord with its higher IPCEs, both at 400–500 nm and in the NIR region, than those of the SQ1-based cell (Figure 4b); the higher IPCEs can be ascribed to HSQ1's higher light-harvesting efficiency

Table 2. Photovoltaic parameters of DSCs based on N3 and on dye cocktails composed of N3 and SQ1 or N3 and HSQ1.

Dyes	IPCE [%] (at nm)	J_{SC} [mA cm^{-2}]	V_{OC} [V]	*FF*	η [%]	Amount of N3 [$\times 10^{-7}$ mol cm^{-2}]	Amount of squaraine dye [$\times 10^{-7}$ mol cm^{-2}]
SQ1	68 (650)	8.98	0.50	0.67	3.01		1.01
HSQ1	71 (700)	11.84	0.55	0.63	4.10		1.19
N3	74 (540), 41 (700)	14.33	0.65	0.70	6.52	1.32	
N3+SQ1	76 (540), 37 (700)	14.64	0.56	0.72	5.90	1.23	0.05
N3+HSQ1	83 (540), 66 (700)	15.76	0.68	0.76	8.14	1.28	0.12

at these wavelengths. Remarkably, the HSQ1 cell exhibited a broad IPCE spectrum (from 400 to 800 nm) with a maximum of 71% at 700 nm; this photoresponse is higher than the photoresponses of all other known squaraine dyes in this long-wavelength region. The V_{OC} of the HSQ1-based cell significantly increased (by 50 mV) compared with that of the SQ1-based cell. HSQ1 and SQ1 possess similar molecular volumes and geometrical structures, but the amount of HSQ1 adsorbed on the TiO_2 surface was about 18% higher than the amount of adsorbed SQ1 (1.19×10^{-7} mol cm^{-2} vs. 1.01×10^{-7} mol cm^{-2}). Therefore, the *cis*-configured HSQ1 could cover much more of the surface than the *trans*-configured SQ1, and the greater coverage can be expected to have kept I_3^- far from the TiO_2 surface, effectively reducing electron recombination and thus increasing V_{OC}. Furthermore, when HSQ1 was adsorbed on the TiO_2 surface, the central squarate oxygen was surrounded by the four methyl groups of the neighbor indolium groups, and the resulting steric crowding likely suppressed back electron transfer (BET) from the TiO_2 to the oxidized dye molecules and improved cell performance. These favorable material properties make HSQ1 potentially useful as a NIR co-sensitizer for dye-cocktail systems.

2.6. Photovoltaic Performance of DSCs Based on Co-Sensitization of N3 and HSQ1

We prepared solar cells co-sensitized with HSQ1 and N3. These two dyes have complementary absorption properties, and HSQ1 has a high photoresponse in the wavelength region between 650 and 750 nm and excellent cell performance. Therefore, we expected co-sensitization to increase the IPCE of N3 in this region and thus lead to a higher energy-conversion efficiency for the resulting DSC. The co-sensitized solar cells were fabricated by immersing TiO_2 films for 24 h in a solution of N3 and HSQ1 or N3 and SQ1 at a molar ratio of 1:1 (0.1 mM for each dye).[14] As expected, the performance of the DSC co-sensitized with HSQ1 and N3 was substantially better than that of the cell based on N3 alone (Table 2 and **Figure 5**). The J_{SC} value increased from 14.33 to 15.76 mA cm^{-2}, V_{OC} increased from 0.65 to 0.68 V, and the fill factor (*FF*) increased slightly, from 0.70 to 0.76. An η value of 8.14% was achieved, which, to our best knowledge, is the highest η reported for a solar cell without utilizing Al_2O_3 layer co-sensitized with a squaraine dye and a ruthenium dye or a metal-free organic dye.[7c] Moreover, this is the first time the IPCE spectrum of N3 at around 700 nm was successfully improved by means of the co-sensitization method without a concomitant decrease in V_{OC}; the IPCE value for the co-sensitized cell was 66% at 700 nm, as compared to 41% for a cell sensitized by N3 alone. In contrast, for a reference cell co-sensitized with N3 and SQ1, J_{SC} increased by only 0.31 mA cm^{-2}, which is consistent with the slight increase of IPCE at around 540 nm and 660 nm; however, the V_{OC} and η values of this cell were only 0.56 V and 5.90%, respectively.

The substantial increase in J_{SC} observed for the DSC co-sensitized with N3 and HSQ1 was in accordance with the improvement of photoresponse over the whole wavelength region in the IPCE spectrum. In the spectrum, the enhancement in the region at around 500 nm was larger than that in other regions, even though this region corresponds to a valley in the HSQ1 absorption spectrum. There are two plausible explanations for this discrepancy. First, HSQ1 may have improved the more uniformly distributed adsorption state of N3 on the TiO_2 film and facilitated the breakup of dye aggregates. We observed similar results in our previous study of a small-molecule co-adsorbent Y1, which effectively prevents dye aggregation and reduces charge recombination in a co-sensitization system.[4a] Second, HSQ1 may have accelerated the regeneration of N3 and suppressed BET from TiO_2 to oxidized N3 ($N3^{\bullet+}$). This possibility is supported by a report indicating that a symmetrical squaraine dye effectively regenerates N3 from its $N3^{\bullet+}$ state and suppresses BET from TiO_2 to $N3^{\bullet+}$ (which occurs on a timescale of microseconds to milliseconds), owing to the faster rate of dye regeneration by squaraine (which occurs on a picosecond timescale).[15] Moreover, the timescale of the aforementioned regeneration process was substantially shorter than that of $N3^{\bullet+}$ reduction by the I^-/I_3^- redox couple (≈10 ns), which means that a small amount of squaraine dye could effectively enhance the

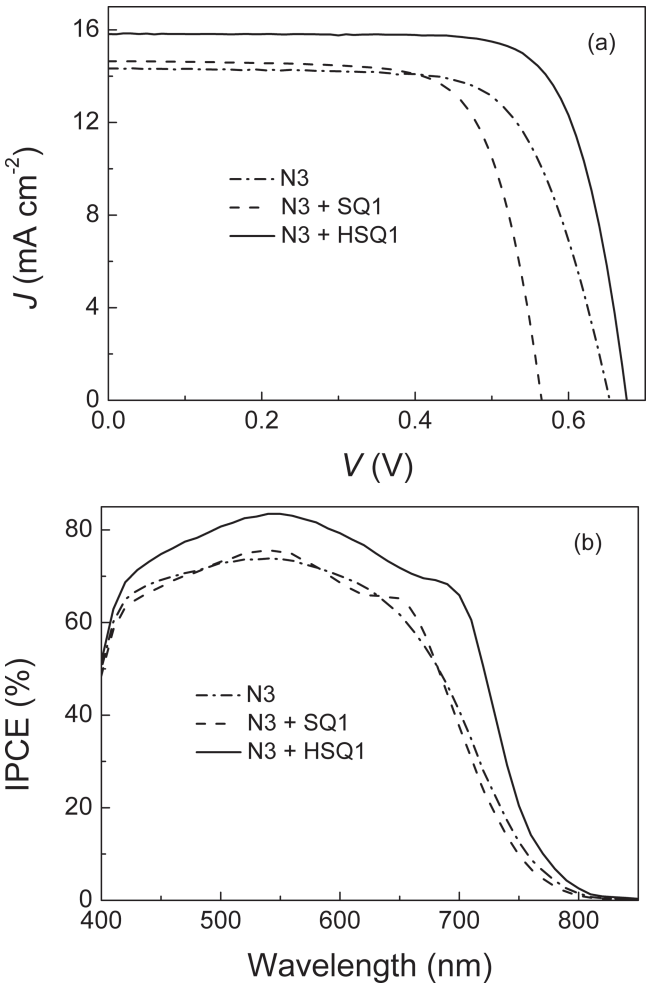

Figure 5. a) *J–V* curves and b) IPCE spectra for DSCs sensitized with N3 and co-sensitized with N3 and SQ1 or with N3 and HSQ1 in an electrolyte composed of 0.6 M dimethylpropyl-imidazolium iodide, 0.05 M I_2, 0.05 M 4-*tert*-butylpyridine, and 0.1 M LiI in acetonitrile.

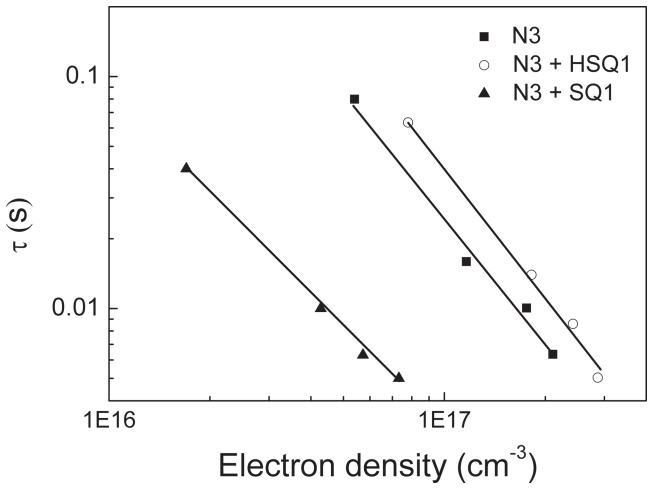

Figure 6. Electron lifetime (τ) as a function of electron density for DSCs sensitized with N3 and co-sensitized with N3 and HSQ1 or with N3 and SQ1.

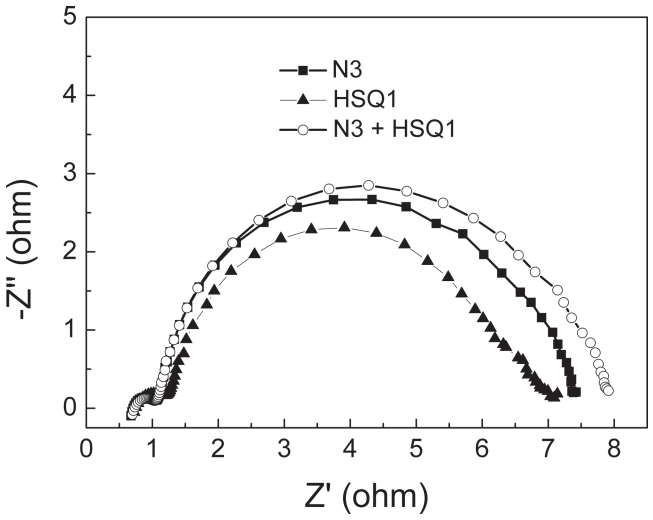

Figure 7. Electrochemical impedance spectroscopy Nyquist plots for DSCs sensitized with N3 and co-sensitized with N3 and HSQ1 or N3 and SQ1.

performance of the co-sensitized solar cells, owing to the faster dye regeneration rate. This kinetic regeneration process was energetically favorable in the system co-sensitized with HSQ1 and N3, owing to the higher redox potential of HSQ1 (0.93 V vs. NHE) relative to that of N3 (1.09 V vs. NHE); such high efficient regeneration likely led to the significant enhancement of IPCE in the range of 400–650 nm and particularly at 540 nm, at which a 12% increase was observed. Furthermore, the remarkable improvement of IPCE at wavelengths exceeding 650 nm can be attributed to the high IPCE response of HSQ1, which resulted from its strong light-harvesting efficiency in this region (ε ~ 202 000 M^{-1} cm^{-1} at 686 nm). Therefore, HSQ1 is an excellent co-sensitizer because a small amount of HSQ1 was sufficient to increase the photoresponse in the NIR region (Table 2).

The V_{OC} of the cell co-sensitized with HSQ1 and N3 was also higher than that of the N3-based cell. To investigate the reason for the differences between the V_{OC} values, we measured the electron lifetime (τ, which reflects the degree of electron recombination) and the electron density of the TiO_2 conduction band of the three DSCs at four bias light intensities by means of intensity-modulated photovoltage spectroscopy and a charge-extraction method, respectively.[16] Plots of the relationship between τ and electron density in the three cells under open-circuit conditions showed that τ increased in the order N3+SQ1 < N3 < N3+HSQ1 (**Figure 6**). This result suggests that HSQ1 and N3 may have formed the best blocking layer between the TiO_2 and the electrolyte, leading to the most effective suppression of charge recombination between the injected electron in the TiO_2 conduction band and I_3^- in the electrolyte. The effective suppression was reflected in the improved V_{OC} and the resulting substantially enhanced energy-conversion efficiency of the cell co-sensitized with HSQ1 and N3. In contrast, the V_{OC} of the co-sensitized cell with N3 and SQ1 (0.56 V) was lower than that of the N3-based cell, owing to a large decrease in the electron lifetime in the TiO_2 film.

In Nyquist plots of the cells based on N3 alone, N3 and HSQ1, and N3 and SQ1 (**Figure 7**), the large semicircles were assigned to the electron transfer resistance (R_{CT}) at the TiO_2/dye/electrolyte interface.[17] Among the three DSCs, the DSC co-sensitized with N3 and HSQ1 showed the largest R_{CT}, suggesting that the electron recombination resistance was increased by co-sensitization with HSQ1. This result also supports our explanation of the high V_{OC} observed for the cell co-sensitized with HSQ1 and N3. Taken together, our results indicate that introduction of the strongly electron-withdrawing dicyanovinyl group into the *cis*-configured squaraine sensitizer not only dramatically improved light-harvesting efficiency but also greatly increased the electron lifetime in the TiO_2 film, as reflected in the improvements in J_{SC}, V_{OC}, and η.

We suggest the following mechanism for the influence of HSQ1 on the performance of the co-sensitized DSC devices (**Figure 8**). First, owing to the *cis*-configuration of HSQ1, the central squarate oxygen was surrounded by the four methyl groups of the indolium groups, and the resulting crowding efficiently suppressed the rate of BET from TiO_2 to the excited state of the dye, relative to the rate for SQ1. Second, the HOMO

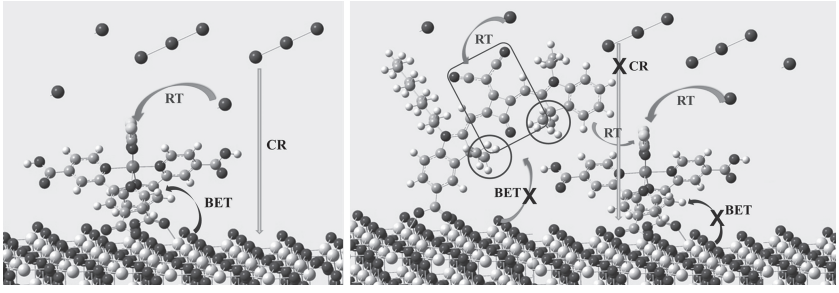

Figure 8. Possible mechanism for improvement of the performance of solar cells by co-sensitization with N3 and HSQ1 dyes: N3 alone (left) and HSQ1+N3 (right). BET, back electron transfer; RT, regeneration; CR, charge recombination.

moiety of HSQ1 was exposed to the electrolyte to a greater degree than the HOMO of SQ1, which may have led to more-efficient regeneration of HSQ1 than of SQ1. These two factors favored the good performance of HSQ1 in both single-dye-based cells and co-sensitized cells. Third, when HSQ1 was used as a co-sensitizer with N3, HSQ1 may also have reduced the BET reaction of N3 and suppressed charge recombination to some degree, as well as accelerated regeneration of N3. Therefore, the cell co-sensitized with N3 and HSQ1 had a higher η than a cell sensitized with N3 alone.

3. Conclusions

We demonstrated that the *cis*-configured squaraine sensitizer HSQ1 had a remarkably red-shifted absorption maximum (to 686 nm) owing to functionalization of the squaric acid core with a strongly electron-withdrawing dicyanovinyl substituent. In addition, a favorable broadening of the absorption spectrum in both the blue and the NIR regions was observed when HSQ1 was adsorbed on TiO_2. A DSC based on HSQ1 showed a broader IPCE spectrum and better performance than an SQ1-based cell under the same conditions. Furthermore, HSQ1 was an excellent co-sensitizer for N3 because it suppressed N3 aggregation, reduced charge recombination, and accelerated regeneration of N3. A DSC co-sensitized with N3 and HSQ1 showed a high IPCE across the entire wavelength region from 400 to 800 nm, with a maximum IPCE value of 66% at 700 nm. An η value of 8.14% was achieved as a result of improvements in both J_{SC} and V_{OC}. Our results demonstrate the great potential of *cis*-configured squaraines as NIR sensitizers and co-sensitizers for DSCs.

4. Experimental Section

Synthesis: All chemicals and reagents were used as received from suppliers without further purification. SQ1, triethylammonium 2-[(1-ethyl-3,3-dimethyl-1,3-dihydro-2*H*-indol-2-ylidene)methyl]-3-(dicyanomethylidene)-4-oxo-cyclobut-1-en-1-olate and 5-carboxyl-2,3,3-trimethyl-1-octyl-3*H*-indolium were synthesized according to the reported method[9a,18]. Column chromatography was performed using Wakogel-C300 as a stationary phase.

3-Cyanoimino-2-(5-carboxy-3,3-dimethyl-1-ethyl-2,3-dihydro-1*H*-2-indolylidenmethyl)-4-(3,3-dimethyl-1-octyl-3*H*-2-indoliumyl-methylene)-1-cyclobuten-1-olate (HSQ1): A mixture of triethylammonium 2-[(1-ethyl-3,3-dimethyl-1,3-dihydro-2*H*-indol-2-ylidene)methyl]-3-(dicyanomethylidene)-4-oxocyclobut-1-en-1-olate (0.48 g, 1 mmol) and 5-carboxyl-2,3,3-trimethyl-1-octyl-3*H*-indolium (0.44 g, 1 mmol) was refluxed with a Dean-Stark apparatus for 12 h in a mixture of toluene-butanol (1:1 v/v, 50 mL) under argon. After removal of the solvent under reduced pressure, the residue was purified by column chromatography on silica gel (methanol/chloroform, 1/20, v/v) to yield a violet solid (0.61 g, 75% yield). ^{1}H NMR (600 MHz, DMSO-d_6 δ): 8.03 (d, J = 1.8 Hz, 1H), 7.97 (dd, J = 8.4 Hz, J = 1.2 Hz, 1H), 7.60 (d, J = 7.2 Hz, 1H), 7.52 (d, J = 7.8 Hz, 1H), 7.44 (m, 2H), 7.33 (d, J = 7.8 Hz, 1H), 6.41 (s, 1H), 6.31 (s, 1H), 4.16 (s, 2H), 4.01 (s, 2H), 1.71 (m, 12H), 1.37 (m, 2H), 1.30 (m, 5H), 1.22 (m, 8H), 0.83 (t, J = 7.2 Hz, 3H). ^{13}C NMR (150 MHz, DMSO-d_6 δ): 173.17, 172.81, 170.76, 167.55, 166.92, 166.61, 163.83, 145.66, 142.86, 142.02, 130.67, 128.82, 125.97, 123.59, 122.92, 118.75, 112.02, 110.73, 89.25, 88.86, 50.05, 48.88, 44.19, 31.56, 29.10, 28.98, 27.08, 26.62, 26.30, 26.03, 22.51, 14.41, 12.56. HRMS (ESI) m/z: $[M-H]^-$ calcd for $C_{40}H_{44}N_4O_3$, 627.33406; found, 627.33436. Anal. calcd for $C_{40}H_{44}N_4O_3$: C 76.40, H 7.05, N 8.91; found: C 76.17, H 7.07, N 8.86. IR (KBr): v = 2920 (COOH), 2190 (CN), 2174 (CN), 1726 (CO), 1678, 1624 cm^{-1}.

Measurement and Characterization: UV-vis-NIR spectra were measured in DMF solution or on a TiO_2 film (thickness = 3.5 μm) with a UV-vis-NIR spectrophotometer (UV-3600, Shimadzu). ^{1}H (600 MHz) and ^{13}C NMR (150 MHz) spectra were measured with a DRX-600 spectrometer (Bruker BioSpin). Mass spectra were measured on a Shimadzu Electrospray ionization (ESI) mass spectrometer. Cyclic voltammetry was performed on a CH Instruments 624D potentiostat/galvanostat system with a three-electrode cell consisting of a Ag/AgCl reference electrode, a working electrode, and a platinum wire counter-electrode. The redox potentials of the dyes were measured in DMF containing 0.1 M tetra-*n*-butylammonium hexafluorophosphate at a scan rate of 100 mV s^{-1}. The geometry and electronic properties of the dyes were performed with the Gaussan09 program package.[19] All calculations were performed by Gaussian software using density functional theory (DFT) with B3LYP/6-31G(d) basis set.

Dye-Sensitized Solar Cells: The DSCs were fabricated as follows. A double-layer TiO_2 photoelectrode (thickness 13 μm; area 0.25 cm^2) was used as a working electrode. An 8 μm transparent layer with titania particles (≈20 nm) and a 5 μm scattering layer with titania particles (≈400 nm) were screen-printed on the fluorine-doped tin oxide conducting glass substrate. A solution of HSQ1 or SQ1 (2×10^{-4} M) and deoxycholic acid (10 mM) in acetonitrile/*tert*-butyl alcohol (1/1, v/v) was used to coat the TiO_2 film with the dye. The electrodes were immersed in the dye solutions and then kept at 35 °C for 4 h to adsorb the dye onto the TiO_2 surface. To co-sensitized DSCs, the TiO_2 electrode was immersed into 1:1 molar ratio of two sensitizers (total concentration = 0.2 mM) with deoxycholic acid (10 mM) for 24 h. The dye-coated TiO_2 film was used as the working electrode, and platinum-coated conducting glass was used as the counter-electrode. The two electrodes were separated by a Surlyn spacer (50 μm thick) and sealed up by heating the polymer frame. The optimized electrolytes were composed of 0.6 M dimethylpropylimidazolium iodide, 0.05 M I_2 and 0.1 M LiI in acetonitrile for only SQ1 or HSQ1; and 0.6 M dimethylpropylimidazolium iodide, 0.05 M I_2, 0.1 M LiI, and 0.05 M 4-*tert*-butylpyridine in acetonitrile for co-sensitization SQ1 or HSQ1 and N3 sensitized solar cells.

Dye Desorbing: N3 was desorbed from the TiO_2 film by immersing in 0.1 M NaOH solution (1:1 mixture of H_2O and ethanol). SQ1 and HSQ1 were desorbed by immersing the TiO_2 film in acetic anhydride for 6 h. Coadsorbed dyes were desorbed by immersing the TiO_2 film in acetic anhydride and 0.1 M NaOH solution (1:1 mixture of H_2O and ethanol), respectively. The amount of adsorbed dye was estimated from the absorption peak of each resulting solution.

Photovoltaic Measurements: The current-voltage characteristics were measured using a black metal mask with an aperture area of 0.2304 cm^2 under standard AM 1.5 G sunlight (100 mW cm^{-2}, WXS-155S-10: Wacom Denso Co. Japan). Monochromatic incident photon-to-current conversion efficiency spectra were measured with monochromatic incident light of 1×10^{16} photons cm^{-2} under 100 mW cm^{-2} in director current mode (CEP-2000BX, Bunko-Keiki).

Intensity-Modulated Photovoltage Spectroscopy: The intensity-modulated photovoltage spectra were measured with a potentiostat (Solartron1287) equipped with a frequency response analyzer (Solartron1255B) at an open-circuit condition based on a monochromatic illumination (420 nm) controlled by Labview system to obtain the photovoltaic response induced by the modulated light. The modulated light was driven with a 10% AC perturbation current super imposed on a DC current in a frequency range from 0.1 to 10^6 Hz.

Charge Extraction Method: The charge extraction method was performed with the same monochromatic light source. The solar cell was illuminated at an open-circuit condition for 5 s to attain a steady state and then the light source was switched off when the device simultaneously switched to a short-circuit condition to extract the charges generated at that light intensity. The electrochemical impedance spectra were measured with an impedance analyzer (Solartron Analytical, 1255B) connected with a potentiostat (Solartron Analytical, 1287) under illumination using a solar simulator (WXS-155S-10: Wacom Denso Co. Japan).

Electrochemical Impedane Spectroscopy: EIS spectra were recorded over a frequency range of 10^{-2}–10^{6} Hz at 298 K. The applied bias voltage and AC amplitude were set at *V*oc of the DSCs. The electrical impedance spectra were characterized using *Z*-View software (Solartron Analytical).

Supporting Information

Supporting Information is available from the Wiley Online Library or from the author.

Acknowledgements

This work was supported by Core Research for Evolutional Science and Technology of the Japan Science and Technology Agency.

Received: November 19, 2012
Revised: December 26, 2012
Published online: February 28, 2013

[1] B. O'Regan, M. Grätzel, *Nature* **1991**, *353*, 737.

[2] a) C. Y. Lee, C. She, N. C. Jeong, J. T. Hupp, *Chem. Commun.* **2010**, *46*, 6090; b) C. Qin, W. Peng, K. Zhang, A. Islam, L. Han, *Org. Lett.* **2012**, *10*, 2532; c) K. Funabiki, H. Mase, A. Hibino, N. Tanaka, N. Mizuhata, Y. Sakuragi, A. Nakashima, T. Yoshida, Y. Kubota, M. Matsui, *Energy Environ. Sci.* **2011**, *4*, 2186; d) C. Qin, A. Islam, L. Han, *Dyes Pigm.* **2012**, *94*, 553; e) T. Bessho, S. M. Zakeeruddin, C.-Y. Yeh, E. W.-G. Diau, M. Grätzel, *Angew. Chem. Int. Ed.* **2010**, *49*, 6646.

[3] a) J.-J. Choi, J.-H. Yum, S.-R. Jang, M. K. Nazeerudin, E. Martinez-Ferrero, E. Palomares, J. Ko, M. Grätzel, T. Torres, *Angew. Chem. Int. Ed.* **2007**, *46*, 8358; b) J.-H. Yum, E. Baranoff, S. Wenger, M. K. Nazeeruddin, M. Grätzel, *Energy Environ. Sci.* **2011**, *4*, 842.

[4] a) L. Han, A. Islam, H. Chen, C. Malapaka, B. Chiranjeevi, S. Zhang, X. Yang, M. Yanagida, *Energy Environ. Sci.* **2012**, *5*, 6057; b) A. Yellla, H.-W. Lee, H. Tsao, C. Yi, A. K. Chandiran, M. K. Nazeerudin, E. W.-G. Diau, C.-Y. Yeh, S. M. Zakeeruddin, M. Grätzel, *Science* **2011**, *334*, 629.

[5] a) C. Jiao, N. Zu, K.-W. Huang, P. Wang, J. Wu, *Org. Lett.* **2011**, *13*, 3652; b) A. Burke, L. Schmidt-Mende, S. Ito, M. Grätzel, *Chem. Commun.* **2007**, *3*, 234.

[6] a) T. Geiger, S. Kuster, J.-H. Yum, S.-J. Moon, M. K. Nazeeruddin, M. Grätzel, F. Nüeesch, *Adv. Funct. Mater.* **2009**, *19*, 2720; b) A. Otsuka, K. Funabiki, N. Sugiyama, T. Yoshida, M. Minoura, M. Matsui, *Chem. Lett.* **2006**, 666; c) J.-H. Yum, P. Walter, S. Huber, D. Rentsch, T. Geiger, F. Nuësch, F. D Angelis, M. Grätzel, M. K. Nazeeruddin, *J. Am. Chem. Soc.* **2007**, *129*, 10320; d) Y. Shi, R. B. M. Hill, J-H. Yum, A. Dualeh, S. Barlow, M. Grätzel, S. R. Marder, M. K. Nazeeruddin, *Angew. Chem. Int. Ed.* **2011**, *50*, 6619.

[7] a) J.-H. Yum, S.-R. Jang, P. Walter, T. Geiger, F. Nüesch, S. Kim, J. Ko, M. Grätzel, M. K. Nazeeruddin, *Chem. Commun.* **2007**, *43*, 4680; b) P. J. Holliman, M. L. Davies, A. Connell, B. V. Velasco, T. M. Watson, *Chem. Commun.* **2010**, *46*, 7256; c) H. Choi, S. Kim, S. O. Kang, J. Ko, M.-S. Kang, J. N. Clifford, A. Forneli, E. Palomares, M. K. Nazeeruddin, M. Grätzel, *Angew. Chem. Int. Ed.* **2008**, *47*, 8259.

[8] a) S. Kuster, F. Sauvage, M. K. Nazeeruddin, M. Grätzel, F. A. Nüesch, T. Geiger, *Dyes Pigm.* **2010**, *87*, 30; b) J.-Y. Li, C.-Y. Chen, C.-P. Lee, S.-C. Chen, T.-H. Lin, H.-H. Tsai, K.-C. Ho, C.-G. Wu, *Org. Lett.* **2010**, *12*, 5454; c) T. Maeda, Y. Hamamura, K. Miyanaga, N. Shima, S. Yagi, H. Nakazumi, *Org. Lett.* **2011**, *12*, 5994.

[9] L. Beverina, R. Ruffo, C. Mari, G. A. Pagani, M. Sassi, F. De Angelis, S. Fantacci, J.-H. Yum, M. Grätzel, M. K. Nazeeruddin, *ChemSusChem* **2009**, *2*, 621.

[10] a) U. Mayerhöffer, K. Deing, K. Gruβ, H. Braunschweig, K. Meerholz, F. Würthner, *Angew. Chem. Int. Ed.* **2009**, *48*, 8776; b) U. Mayerhöffer, B. Fimmel, F. Würthner, *Angew. Chem. Int. Ed.* **2012**, *51*, 164.

[11] G. Oskam, B. V. Bergeron, G. J. Meyer, P. C. Searson, *J. Chem. Chem. B* **2001**, *105*, 6867.

[12] A. Hagfeld, M. Grätzel, *Chem. Rev.* **1995**, *95*, 49.

[13] a) N. Koide, L. Han, *Rev. Sci. Instrum.* **2004**, *75*, 2828; b) N. Koide, Y. Chiba, L. Han, *Jpn. J. Appl. Phys.* **2005**, *44*, 4176; c) X. Yang, M. Yanagida, L. Han, *Energy Environ. Sci.* **2012**, *6*, 54.

[14] Using different dye concentrations, we found that the optimum molar ration of HSQ1 and N3 for achieving highest efficiency is 1 to 1.

[15] P. Zhang, C. Li, Y.-S. Wu, X.-C. Ai, X.-S. Wang, B.-W. Zhang, J.-P. Zhang, *J. Photochem. Photobiol., A* **2006**, *183*, 138.

[16] a) N. W. Duffy, L. M. Peter, R. M. G. Rajapakse, K. G. U. Wijayantha, *J. Phys. Chem. B* **2000**, *104*, 8916; b) G. Schlichthoerl, S. Y. Huang, J. Sprague, A. J. Frank, *J. Phys. Chem. B* **1997**, *101*, 8141.

[17] L. Han, N. Koide, Y. Chiba, T. Mitate, *Appl. Phys. Lett.* **2004**, *84*, 2433.

[18] A. L. Tatarets, I. A. Fedyunyaeva, E. Terpetshnig L. D. Patsenker, *Dyes Pigm.* **2005**, *64*, 125.

[19] M. J. Frisch, G. W. Trucks, H. B. Schlegel, G. E. Scuseria, M. A. Robb, J. R. Cheeseman, G. Scalmani, V. Barone, B. Mennucci, G. A. Petersson, H. Nakatsuji, M. Caricato, X. Li, H. P. Hratchian, A. F. Izmaylov, J. Bloino, G. Zheng, J. L. Sonnenberg, M. Hada, M. Ehara, K. Toyota, R. Fukuda, J. Hasegawa, M. Ishida, T. Nakajima, Y. Honda, O. Kitao, H. Nakai, T. Vreven, J. A. Montgomery, J. E. Peralta, F. Ogliaro, M. Bearpark, J. J. Heyd, E. Brothers, K. N. Kudin, V. N. Staroverov, R. Kobayashi, J. Normand, K. Raghavachari, A. Rendell, J. C. Burant, S. S. Iyengar, J. Tomasi, M. Cossi, N. Rega, N. J. Millam, M. Klene, J. E. Knox, J. B. Cross, V. Bakken, C. Adamo, J. Jaramillo, R. Gomperts, R. E. Stratmann, O. Yazyev, A. J. Austin, R. Cammi, C. Pomelli, J. W. Ochterski, R. L. Martin, K. Morokuma, V. G. Zakrzewski, G. A. Voth, P. Salvador, J. J. Dannenberg, S. Dapprich, A. D. Daniels, O. Farkas, J. B. Foresman, J. V. Ortiz, J. Cioslowski, D. J. Fox, Gaussian 09 A.2 Revision, Gaussian, Inc., Wallingford, CT **2009**.